Journal of Human Genetics (2018) 63:1197–1210
https://doi.org/10.1038/s10038-018-0510-3

ARTICLE

Molecular pathogenesis of triple-negative breast cancer based on microRNA expression signatures: antitumor *miR-204-5p* targets *AP1S3*

Hiroko Toda[1] · Sasagu Kurozumi[2] · Yuko Kijima[1] · Tetsuya Idichi[1] · Yoshiaki Shinden[1] · Yasutaka Yamada[3] · Takayuki Arai[3] · Kosei Maemura[1] · Takaaki Fujii[2] · Jun Horiguchi[4] · Shoji Natsugoe[1] · Naohiko Seki[3]

Received: 19 July 2018 / Revised: 20 August 2018 / Accepted: 22 August 2018 / Published online: 18 September 2018

Abstract

Triple-negative breast cancer (TNBC) is an aggressive type of cancer associated with a poor prognosis. Identification of novel therapeutic targets in TNBC is urgently needed. Here, we investigated the microRNA (miRNA) expression signature of TNBC using clinical specimens. In total, 104 miRNAs (56 upregulated and 48 downregulated) were significantly dysregulated in TNBC tissues; *miR-204-5p* showed the most dramatic downregulation. We then examined the antitumor roles of *miR-204-5p* in breast cancer (BC) cells. Notably, cancer cell migration and invasion were significantly reduced by ectopic expression of *miR-204-5p* in BC cells. Genome-wide gene expression analysis and in silico database search revealed that 32 genes were putative *miR-204-5p* targets. High expression of *AP1S3*, *RACGAP1*, *ELOVL6*, and *LRRC59* was significantly associated with poor prognosis in patients with BC, and adaptor-related protein complex 1 sigma 3 subunit (*AP1S3*) was directly regulated by *miR-204-5p*, as demonstrated by luciferase reporter assays. *AP1S3* overexpression was detected in TNBC clinical specimens and enhanced cancer cell aggressiveness. We further analyzed downstream RNA networks regulated by *AP1S3* in BC cells. Overall, this miRNA signature is expected to be an effective tool for identification of miRNA-mediated molecular mechanisms of TNBC pathogenesis.

Introduction

Despite advances in early detection systems and currently developed molecular targeted therapies, breast cancer (BC) is a leading cause of cancer-related death among women in industrialized countries [1, 2]. Based on the St. Gallen Consensus Meeting of Breast Cancer, BC can be classified into five subtypes as follows: luminal A-like type, luminal B-like type, hormone receptor-positive and human epidermal growth factor receptor 2 (HER2)-positive type, hormone receptor-negative and HER2-postive type, and triple-negative type [3–5]. Triple-negative BC (TNBC) includes tumors without the expression of estrogen receptor (ER), progesterone receptor (PR), and HER2 and largely overlaps with the basal subtype, representing only 15–20% of BC cases [3–5]. Due to the aggressive nature of TNBC and the lack of novel targeted therapies, TNBC has a significantly worse prognosis than other types of BC [6, 7]. Recent genomic approaches have offered the possibility to improve treatment approaches through the identification of novel targets for TNBC anticancer therapy.

MicroRNAs (miRNAs) are small noncoding RNAs that fine-tune the expression of protein coding/noncoding RNAs by repressing translation or cleaving RNA transcripts in a

Electronic supplementary material The online version of this article (https://doi.org/10.1038/s10038-018-0510-3) contains supplementary material, which is available to authorized users.

✉ Naohiko Seki
naoseki@faculty.chiba-u.jp

[1] Department of Digestive Surgery, Breast and Thyroid Surgery, Graduate School of Medical and Dental Sciences, Kagoshima University, Kagoshima, Japan

[2] Department of General Surgical Science, Gunma University Graduate School of Medicine, Gunma, Japan

[3] Department of Functional Genomics, Chiba University Graduate School of Medicine, Chiba, Japan

[4] Department of Breast Surgery, International University of Health and Welfare, Chiba, Japan

sequence-dependent manner [8, 9]. Many studies have shown that miRNAs play important roles in various physiological processes, such as cell differentiation, proliferation, and apoptosis [10, 11]. In humans, dysregulation of miRNAs is associated with many human diseases, including BC pathogenesis [12–14]. Based on the unique nature of miRNA biology, a single miRNA controls many RNA transcripts in normal and diseased cells [9, 15]. Identification of aberrantly expressed miRNAs in cancer cells is the first step for elucidation of miRNA-mediated cancer pathways.

Advanced RNA sequencing technologies are suitable for construction of miRNA expression signatures. We have provided miRNA expression signatures based on RNA sequencing in several cancer types, e.g., bladder cancer, castration-resistant prostate cancer, pancreatic cancer, and head and neck cancer [16–19]. In this study, we created the miRNA expression signature of TNBC by RNA sequencing using clinical specimens and found that 104 miRNAs (56 upregulated and 48 downregulated) were significantly dysregulated in TNBC tissues. These dysregulated miRNAs represent an important starting point for elucidation of the molecular pathology of TNBC.

Our signature showed that *miR-204-5p* was significantly downregulated in TNBC tissues. Therefore, we aimed to identify targets of *miR-204-5p* involved in TNBC pathogenesis. Identification of aberrantly expressed miRNA-mediated cancer networks is expected to provide insights into the potential mechanisms underlying TNBC pathogenesis and to facilitate the establishment of novel therapeutic targets.

Materials and methods

Patients, BC specimens, and cell lines

Thirty-five clinical tissue specimens were collected from patients with BC who underwent surgical resection at Gunma University Hospital and Kagoshima University Hospital between 2003 and 2018. The clinicopathological features of patients with BC are shown in Supplementary Table 1. All patients in this study provided informed consent, and the study protocol was approved by the Institutional Review Board of Gunma University (approval nos. 2016-023 and 2017-163) and Kagoshima University (approval no. 28-65).

MDA-MB-231 and MDA-MB-157 cells were used in this study. All cell lines were obtained from Public Health England (Salisbury, UK).

Total RNA, including miRNA, was isolated using TRIzol reagent (Invitrogen, Carlsbad, CA, USA).

Construction of the miRNA expression signature for TNBC

Small RNA sequencing was performed using a HiSeq 2000 instrument (Illumina, San Diego, CA, USA) for five TNBC samples and three normal breast epithelial tissue samples (Supplementary Table 1). Small RNA sequencing and data mining procedures were described in our previous studies [16–20].

Quantitative real-time reverse transcription polymerase chain reaction (qRT-PCR)

The procedure for qRT-PCR has been described previously [21–24]. Briefly, the expression levels of miRNAs were analyzed by TaqMan qRT-PCR assays (*miR-204-5p*, assay ID: 000508; Applied Biosystems, Foster City, CA, USA). Data were normalized to *RNU48* (assay ID: 001006; Applied Biosystems). In addition, the expression levels of target genes of *miR-204-5p* were assessed with the following TaqMan probes and primers: *AP1S3*, assay ID: Hs00950999; Applied Biosystems, normalized to *GUSB* (assay ID: Hs00939627_ml; Applied Biosystems).

Effects of transfection with miRNA mimic or small-interfering RNA (siRNA) on cell proliferation, migration, and invasion

The transfection procedures for miRNAs or siRNAs into cancer cells were described previously [21–24]. The following mature miRNAs or siRNAs were used in this study: mature miRNAs (Ambion Pre-miR miRNA precursor; *miR-204-5p*, ID: PM11116; Applied Biosystems), siRNAs (Stealth Select RNAi siRNA; si-*AP1S3*, ID: HSS134239 and HSS134240; Invitrogen), and negative control miRNA/siRNA (product ID: AM17010; Thermo Fisher Scientific, Waltham, MA, USA).

Protocols for determining cell proliferation, migration, and invasion were described previously [21–24].

Genome-wide gene expression and in silico analyses for the identification of genes regulated by *miR-204-5p* in BC cells

Microarray gene expression analysis and in silico analysis were used to identify putative target genes regulated by *miR-204-5p*. The microarray data of *miR-204-5p* transfectants were deposited in the Gene Expression Omnibus (GEO) repository under accession number GSE115801. Gene expression data by microarray analyses of TNBC clinical specimens were deposited in the GEO database

(GSE118539). Putative target genes having a binding site for *miR-204-5p* were detected by TargetScan Human ver.7.1 (http://www.targetscan.org/vert_71/). Our strategy for identification of *miR-204-5p* target genes is outlined in Supplementary Fig. 1.

The Cancer Genome Atlas (TCGA) data analysis

To assess the clinical significance of *miR-204-5p*-targeted genes, we used the RNA sequencing database in TCGA. High and low expression were defined by dividing the clinical data population in half based on the expression level. Gene expression and clinical data were obtained from cBioportal and OncoLnc (data downloaded November 1, 2017). Data mining procedures were described in our previous studies [21–24].

Plasmid construction and dual-luciferase reporter assays

The following sequences were inserted into the psiCHECk-2 vector (C8021; Promega, Madison, WI, USA): the wild-type sequence of the 3′-untranslated region (UTR) of *AP1S3* or the deletion-type, which lacked the *miR-204-5p* binding sites (positions 111−117 or 1993–2000; Fig. 2c, upper panel).

The cloned vectors were cotransfected into MDA-MB-231 cells with mature *miR-204-5p*. The procedures for transfection and dual-luciferase reporter assays were described in previous studies [21–24].

Western blotting and immunohistochemistry

Anti-human AP1S3 rabbit polyclonal IgG (1:500; ab205509; Abcam, Cambridge, UK) was used as a primary antibody. Anti-glyceraldehyde 3-phosphate dehydrogenase (GAPDH) mouse monoclonal IgG (1:2000; SAF6698; Wako, Osaka, Japan) was used as an internal control. The protocol for western blot analysis was described previously [21–24].

Anti-human AP1S3 rabbit polyclonal IgG (1:200; PA5-23894; Thermo Fisher Scientific) was used as a primary antibody for immunohistochemistry. The procedures were described in previous studies [21–24].

Identification of downstream genes regulated by *AP1S3* in BC cells

The microarray data for si-*AP1S3* transfectants were deposited in the GEO repository under accession number GSE115909.

Statistical analysis

Mann−Whitney *U* tests were used to analyze differences between two groups. Bonferroni-adjusted Mann−Whitney *U* tests were used to analyze the differences among more than three groups. Statistical tests were performed using Expert StatView software (version 5.0, SAS Institute Inc., Cary, NC, USA). Survival analysis was performed using the Kaplan–Meier method, log-rank tests, and multivariable Cox hazard regression analyses with JMP software (version 13; SAS Institute Inc., Cary, NC, USA).

Results

Small RNA sequencing of TNBC specimens and construction of miRNA signatures

To create the miRNA expression signature of TNBC, we performed small RNA sequencing of eight RNA libraries (derived from three normal breast epithelial tissues and five TNBC tissues). The clinical features of clinical specimens are summarized in Supplementary Table 1. We obtained between 10,112,225 and 14,568,843 reads in this analysis. After filing and trimming of the sequenced reads, between 7,076,489 and 12,271,020 miRNA reads (larger than 19 nucleotides) were mapped in the human genome (Supplementary Table 2). Human genome-matched sequenced reads were divided into small RNAs according to their biological features (Supplementary Table 2).

We then created the miRNA expression signature that included miRNAs exhibiting significant up- or down-regulation (false discovery rate < 0.05) in TNBC tissues (Table 1). In total, 56 upregulated miRNAs and 48 downregulated miRNAs were detected from aligned reads using R program (Table 1). Among these dysregulated miRNAs, 23 were annotated as passenger strands of miRNAs in the miRBase database (Release 22, http://www.mirbase.org/).

Expression levels of *miR-204-5p* in BC specimens and cell lines

To confirm the miRNA expression signature, expression levels of *miR-204-5p* in normal breast epithelial tissues ($n = 11$), TNBC tissues ($n = 16$), and cell lines (MDA-MB-231 and MDA-MB-157) were evaluated. The expression level of *miR-204-5p* was significantly downregulated in TNBC specimens (Fig. 1a). Additionally, the expression levels of this miRNA in the two cell lines were lower than those in normal BC epithelial specimens (Fig. 1a).

Table 1 Aberrantly expressed miRNAs identified by deep sequencing of TNBC clinical specimens

miRNA	miRBase accession	Chromosome	Log_2FC	*p* value	FDR
(a) Downregulated miRNAs identified by deep sequencing of TNBC clinical specimens					
hsa-miR-204-5p	*MIMAT0000265*	chromosome 9	−5.7466	4.733E-21	1.219E-17
hsa-miR-202-5p	*MIMAT0002810*	chromosome 10	−5.3219	5.735E-06	0.0005998
hsa-miR-139-5p	*MIMAT0000250*	chromosome 11	−4.7757	8.239E-17	1.061E-13
hsa-miR-483-3p	*MIMAT0002173*	chromosome 11	−4.5507	7.176E-07	0.000168
hsa-miR-4703-3p	*MIMAT0019802*	chromosome 13	−4.5027	0.0001721	0.0074831
hsa-miR-135a-5p	*MIMAT0000428*	chromosome 3 chromosome 12	−4.2023	1.249E-06	0.0002148
hsa-miR-944	*MIMAT0004987*	chromosome 3	-4.0504	4.071E-08	2.097E-05
hsa-miR-4510	*MIMAT0019047*	chromosome 15	−4.0019	7.391E-05	0.0040506
hsa-miR-99a-5p	*MIMAT0000097*	chromosome 21	−3.8016	1.904E-07	7.008E-05
hsa-miR-655-3p	*MIMAT0003331*	chromosome 14	−3.7967	1.209E-05	0.0010046
hsa-miR-1247-3p	*MIMAT0022721*	chromosome 14	−3.7056	5.21E-05	0.0029825
hsa-miR-335-5p	*MIMAT0000765*	chromosome 7	−3.7018	1.75E-05	0.0012878
hsa-miR-99a-3p	*MIMAT0004511*	chromosome 21	−3.5885	2.977E-07	9.585E-05
hsa-miR-585-3p	*MIMAT0003250*	chromosome 5	−3.4681	0.0003166	0.0119949
hsa-miR-551b-3p	*MIMAT0003233*	chromosome 3	−3.3990	7.141E-05	0.0039987
hsa-miR-100-5p	*MIMAT0000098*	chromosome 11	−3.1609	2.297E-05	0.0015994
hsa-miR-376a-3p	*MIMAT0000729*	chromosome 14 chromosome 14	−3.1528	6.438E-06	0.0006379
hsa-miR-376c-3p	*MIMAT0000720*	chromosome 14	−3.1368	1.056E-05	0.0009071
hsa-miR-675-3p	*MIMAT0006790*	chromosome 11	−3.0840	0.0001994	0.008211
hsa-miR-195-5p	*MIMAT0000461*	chromosome 17	−3.0433	5.249E-10	4.508E-07
hsa-let-7c-5p	*MIMAT0000064*	chromosome 21	−2.9862	2.498E-06	0.0003574
hsa-miR-144-3p	*MIMAT0000436*	chromosome 17	−2.8769	0.0002415	0.0095713
hsa-miR-26a-5p	*MIMAT0000082*	chromosome 3 chromosome 12	−2.8446	3.101E-06	0.0003994
hsa-miR-451a	*MIMAT0001631*	chromosome 17	−2.8284	0.0001438	0.0066166
hsa-miR-10b-3p	*MIMAT0004556*	chromosome 2	−2.7576	5.135E-06	0.0005752
hsa-miR-30a-3p	*MIMAT0000088*	chromosome 6	−2.7501	7.537E-08	3.236E-05
hsa-miR-126-5p	*MIMAT0000444*	chromosome 9	−2.6694	6.656E-07	0.000168
hsa-miR-190b	*MIMAT0004929*	chromosome 1	−2.6135	0.0002588	0.0100995
hsa-miR-101-5p	*MIMAT0004513*	chromosome 1	−2.6092	1.854E-06	0.000281
hsa-miR-136-3p	*MIMAT0004606*	chromosome 14	−2.6032	0.0001921	0.0081129
hsa-miR-10b-5p	*MIMAT0000254*	chromosome 2	−2.5294	8.19E-06	0.0007813
hsa-miR-145-3p	*MIMAT0004601*	chromosome 5	−2.4632	1.416E-05	0.0011057
hsa-miR-299-3p	*MIMAT0000687*	chromosome 14	−2.3910	0.0005971	0.019469
hsa-miR-497-5p	*MIMAT0002820*	chromosome 17	−2.3457	1.979E-05	0.0014159
hsa-miR-125b-2-3p	*MIMAT0004603*	chromosome 21	−2.3340	0.0016291	0.0423897
hsa-miR-486-5p	*MIMAT0002177*	chromosome 8	−2.2378	0.0005839	0.019282
hsa-miR-193a-3p	*MIMAT0000459*	chromosome 17	−2.2220	0.0008906	0.0263695
hsa-miR-126-3p	*MIMAT0000445*	chromosome 9	−2.1947	2.371E-05	0.0016075
hsa-miR-381-3p	*MIMAT0000736*	chromosome 14	−2.1518	0.0016488	0.0424725
hsa-miR-424-5p	*MIMAT0001341*	chromosome X	−2.1004	0.0001274	0.0059654
hsa-miR-574-3p	*MIMAT0003239*	chromosome 4	−1.9757	3.572E-05	0.0021398
hsa-miR-218-5p	*MIMAT0000275*	chromosome 4 chromosome 5	−1.8904	3.339E-05	0.0020978

Table 1 (continued)

miRNA	miRBase accession	Chromosome	Log_2FC	*p* value	FDR
hsa-miR-143-3p	*MIMAT0000435*	chromosome 5	−1.7688	0.0012403	0.0343544
hsa-miR-195-3p	*MIMAT0004615*	chromosome 17	−1.7473	0.0018771	0.0474065
hsa-miR-152-3p	*MIMAT0000438*	chromosome 17	−1.7274	0.0014724	0.0395089
hsa-miR-30e-3p	*MIMAT0000693*	chromosome 1	−1.6871	0.0005417	0.018122
hsa-miR-101-3p	*MIMAT0000099*	chromosome 1 chromosome 9	−1.6620	0.0003914	0.0138126
hsa-miR-30a-5p	*MIMAT0000087*	chromosome 6	−1.5507	0.0014077	0.0381695
(b) Upregulated miRNAs identifed by deep sequencing of TNBC clinical specimens					
hsa-miR-767-5p	*MIMAT0003882*	chromosome X	7.6754	0.000308	0.011854
hsa-miR-592	*MIMAT0003260*	chromosome 7	6.1661	7.86E-05	0.004219
hsa-miR-4746-5p	*MIMAT0019880*	chromosome 19	5.5509	0.000658	0.020606
hsa-miR-3690	*MIMAT0018119*	chromosome X chromosome Y	4.6420	0.000746	0.022349
hsa-miR-21-3p	*MIMAT0004494*	chromosome 17	4.6367	3.08E-09	1.99E-06
hsa-miR-7977	*MIMAT0031180*	chromosome 3	4.5763	0.001239	0.034354
hsa-miR-183-3p	*MIMAT0004560*	chromosome 7	4.5507	0.000389	0.013813
hsa-miR-187-3p	*MIMAT0000262*	chromosome 18	4.4802	0.001986	0.049195
hsa-miR-362-5p	*MIMAT0000705*	chromosome X	4.0486	8.62E-07	0.000185
hsa-miR-340-3p	*MIMAT0000750*	chromosome 5	3.8616	0.000671	0.020606
hsa-miR-766-3p	*MIMAT0003888*	chromosome X	3.8411	0.000154	0.006855
hsa-miR-3529-3p	*MIMAT0022741*	chromosome 15	3.7651	0.000356	0.013282
hsa-miR-330-5p	*MIMAT0004693*	chromosome 19	3.7624	3.51E-05	0.00214
hsa-miR-301b	*MIMAT0004958*	chromosome 22	3.7427	1.07E-06	0.000213
hsa-miR-1301-3p	*MIMAT0005797*	chromosome 2	3.6743	8.6E-06	0.000786
hsa-miR-92b-3p	*MIMAT0003218*	chromosome 1	3.6644	1.68E-06	0.000271
hsa-miR-877-5p	*MIMAT0004949*	chromosome 6	3.6226	0.000387	0.013813
hsa-miR-7706	*MIMAT0030021*	chromosome 15	3.6051	1.25E-06	0.000215
hsa-miR-7-5p	*MIMAT0000252*	chromosome 9 chromosome 15 chromosome 19	3.5659	9.81E-05	0.004859
hsa-miR-615-3p	*MIMAT0003283*	chromosome 12	3.4688	8.33E-05	0.004294
hsa-miR-3677-3p	*MIMAT0018101*	chromosome 16	3.4646	0.001594	0.041903
hsa-miR-130b-5p	*MIMAT0004680*	chromosome 22	3.3871	0.000522	0.017683
hsa-miR-301a-3p	*MIMAT0000688*	chromosome 17	3.2527	1.3E-05	0.001049
hsa-miR-454-3p	*MIMAT0003885*	chromosome 17	3.1273	3.82E-06	0.000468
hsa-miR-577	*MIMAT0003242*	chromosome 4	3.0976	1.74E-05	0.001288
hsa-miR-210-3p	*MIMAT0000267*	chromosome 11	3.0938	0.001079	0.03089
hsa-miR-454-5p	*MIMAT0003884*	chromosome 17	3.0932	0.00111	0.031434
hsa-miR-589-5p	*MIMAT0004799*	chromosome 7	3.0506	5.82E-06	0.0006
hsa-miR-3607-3p	*MIMAT0017985*	chromosome 5	3.0428	0.000204	0.008211
hsa-miR-93-3p	*MIMAT0004509*	chromosome 7	2.8964	0.000672	0.020606
hsa-miR-142-3p	*MIMAT0000434*	chromosome 17	2.8723	0.000428	0.014903
hsa-miR-1307-3p	*MIMAT0005951*	chromosome 10	2.8493	4E-06	0.000468
hsa-miR-130b-3p	*MIMAT0000691*	chromosome 22	2.8392	5.48E-07	0.000157
hsa-miR-148b-5p	*MIMAT0004699*	chromosome 12	2.7574	0.000174	0.007483
hsa-miR-183-5p	*MIMAT0000261*	chromosome 7	2.7380	0.000149	0.006745
hsa-miR-2467-5p	*MIMAT0019952*	chromosome 2	2.7328	0.001827	0.046609

Table 1 (continued)

miRNA	miRBase accession	Chromosome	Log_2FC	*p* value	FDR
hsa-miR-182-5p	*MIMAT0000259*	chromosome 7	2.7306	0.00012	0.005708
hsa-miR-425-5p	*MIMAT0003393*	chromosome 3	2.7247	2.75E-06	0.000372
hsa-miR-1307-5p	*MIMAT0022727*	chromosome 10	2.7039	0.000681	0.020639
hsa-miR-146b-3p	*MIMAT0004766*	chromosome 10	2.6160	0.000459	0.015758
hsa-miR-15b-5p	*MIMAT0000417*	chromosome 3	2.5758	8.85E-06	0.000786
hsa-miR-500a-3p	*MIMAT0002871*	chromosome X	2.5241	2.72E-05	0.001797
hsa-miR-155-5p	*MIMAT0000646*	chromosome 21	2.5055	0.001062	0.030744
hsa-miR-345-5p	*MIMAT0000772*	chromosome 14	2.4584	5.08E-05	0.002976
hsa-miR-671-3p	*MIMAT0004819*	chromosome 7	2.2793	0.001051	0.030744
hsa-miR-484	*MIMAT0002174*	chromosome 16	2.1711	0.000203	0.008211
hsa-miR-181a-5p	*MIMAT0000256*	chromosome 9 chromosome 1	2.1572	3.22E-05	0.002073
hsa-miR-21-5p	*MIMAT0000076*	chromosome 17	2.1288	0.000102	0.004965
hsa-miR-93-5p	*MIMAT0000093*	chromosome 7	2.0790	9.24E-05	0.004667
hsa-miR-17-3p	*MIMAT0000071*	chromosome 13	2.0487	0.00063	0.020035
hsa-miR-421	*MIMAT0003339*	chromosome X	2.0131	0.000627	0.020035
hsa-miR-181b-5p	*MIMAT0000257*	chromosome 1 chromosome 9	2.0116	8.33E-05	0.004294
hsa-miR-324-5p	*MIMAT0000761*	chromosome 17	1.9996	0.00131	0.035896
hsa-miR-20a-5p	*MIMAT0000075*	chromosome 13	1.9901	0.000389	0.013813
hsa-miR-181c-3p	*MIMAT0004559*	chromosome 19	1.9387	0.001559	0.041395
hsa-miR-181a-3p	*MIMAT0000270*	chromosome 1	1.7713	0.001916	0.04792

The clinical features of patients with TNBC are summarized in Supplementary Table 1.

Effects of restoring *miR-204-5p* on cell proliferation, migration, and invasion in BC cells

To evaluate the antitumor effects of *miR-204-5p*, we applied gain-of-function assays in TNBC cell lines (MDA-MB-231 and MDA-MB-157). Ectopic expression of *miR-204-5p* significantly blocked cancer cell proliferation, migration, and invasion (Fig. 1b–d).

Identification of putative target genes regulated by *miR-204-5p* in BC cells and their clinical significance

To identify putative oncogenic genes regulated by *miR-204-5p* in TNBC cells, we applied three different datasets: (1) candidates of *miR-204-5p* binding genes in the TargetScan database, (2) genes downregulated by *miR-204-5p* transfection in MDA-MB-231 cells (GEO accession number, GSE115801), and (3) our original gene expression data from TNBC clinical specimens. Our strategy for identification of putative target genes regulated by *miR-204-5p* in TNBC cells is shown in Supplementary Fig. 1. Finally, 32 genes were identified as *miR-204-5p*-regulated oncogenes (Table 2). Oligo microarrays (Human GE 60K; Agilent Technologies) were used for gene expression analyses of TNBC clinical specimens. The microarray data were deposited into GEO (https://www.ncbi.nlm.nih.gov/geo/), with accession number GSE118539.

Next, to investigate the clinical significance of these targets, we analyzed the relationships between gene expression and prognosis in patients with BC using TCGA database. Among these targets, high expression levels of four genes (*AP1S3*: $p = 0.00823$, *RACGAP1*: $p = 0.0277$, *ELOVL6*: $p = 0.0448$, and *LRRC59*: $p = 0.0456$) were significantly associated with poor prognosis in patients with BC by TCGA database analyses (Fig. 4c and Supplementary Fig. 2). Expression levels of three genes (*RACGAP1*, *ELOVL6*, and *LRRC59*) were decreased by transfected with *miR-204-5p* into BC cells (Supplementary Fig. 2).

Direct regulation of *AP1S3* by *miR-204-5p* in BC cells

We then examined whether *miR-204-5p* regulated *AP1S3* in TNBC cells. We confirmed that gene expression of *AP1S3* was significantly decreased in TNBC cells transfected with *miR-204-5p* (Fig. 2a). Additionally, western blot analyses revealed that AP1S3 protein levels in TNBC cells were decreased by transfection with *miR-204-5p* (Fig. 2b).

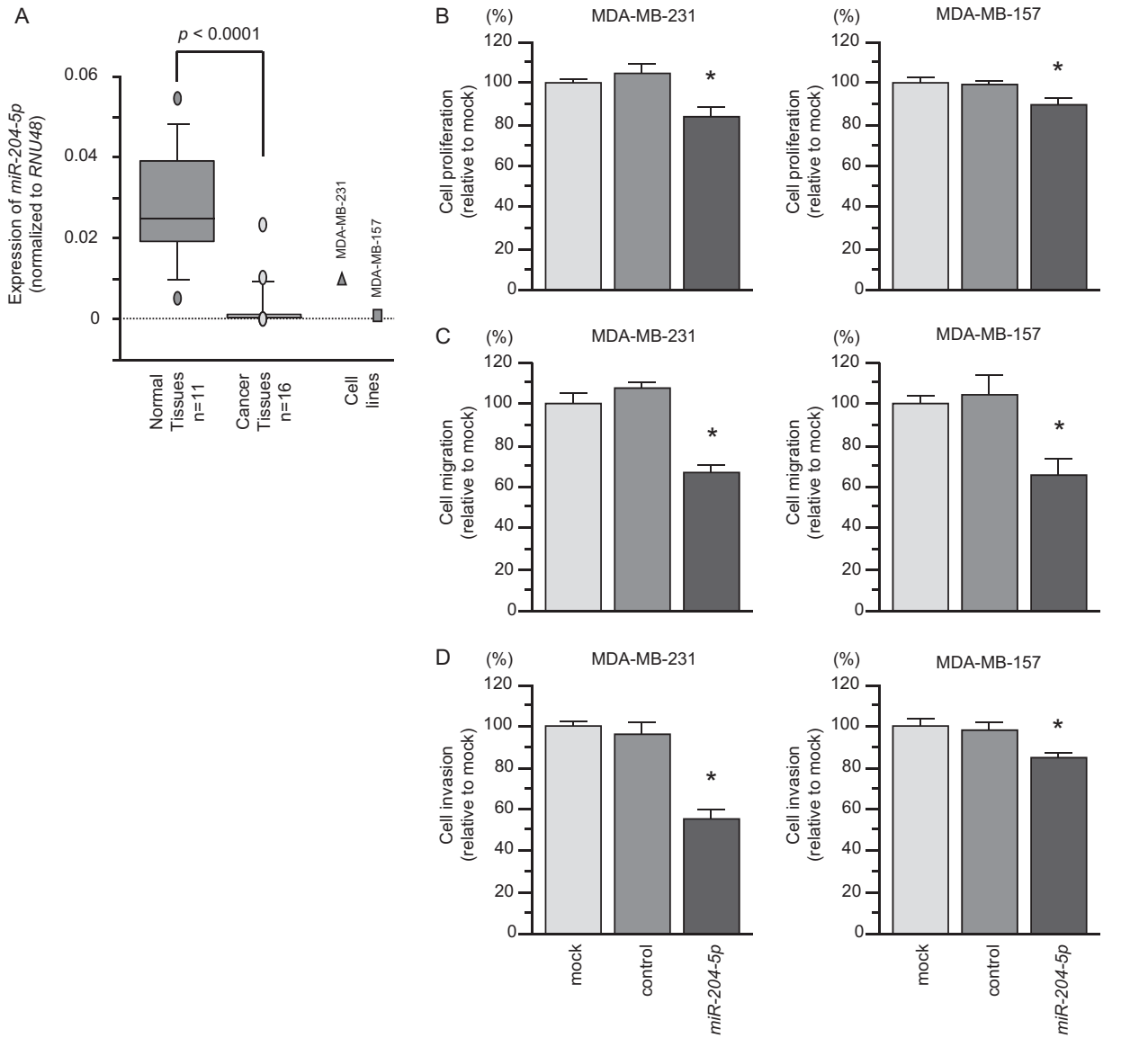

Fig. 1 Effects of ectopic expression of *miR-204-5p* on BC cells. **a** Expression levels of *miR-204-5p* in TNBC clinical specimens and cell lines (MDA-MB-231 and MDA-MB-157). *RNU48* was used as an internal control. **b** Cell proliferation was determined by XTT assays 72 h after transfection with *miR-204-5p p*. $*p < 0.05$. **c** Results of cell migration assays. $*p < 0.05$. **d** Cell invasion activity was determined using Matrigel invasion assays. $*p < 0.05$

Next, we performed luciferase reporter assays with MDA-MB-231 cells to determine whether *miR-204-5p* directly targeted the 3′-UTR of *AP1S3*. According to the TargetScan human database, the binding sites for *miR-204-5p* in the 3′-UTR of *AP1S3* consisted of two regions (positions 111−117 and 1993−2000; Fig. 2c, upper panel).

Moreover, we showed that *miR-204-5p* suppressed reporter activity in cells transfected with the wild-type *AP1S3* vector compared with that in mock or miR-control transfectants ($p < 0.005$, Fig. 2c, lower panel), whereas transfectants of the mutant vector were not decreased. These data indicated that *miR-204-5p* was directly bound to two putative binding sites in the 3′-UTR of *AP1S3*.

In addition, adaptor protein complex 1 (AP-1) consists of three member of genes, *AP1S1*, *AP1S2*, and *AP1S3*. In this study, we identified *AP1S1* and *AP1S2* as putative targets of *miR-204-5p* regulation in BC cells. Expression of *AP1S1* was upregulated in TNBC clinical specimens. *AP1S2* was not upregulated in TNBC clinical specimens (Supplementary Fig. 3A). Expression of *AP1S1* and *AP1S2* was reduced by *miR-204-5p* in BC cells (Supplementary Fig. 3B).

Effects of *AP1S3* knockdown on cell proliferation, migration, and invasion in BC cells

To assess the function of *AP1S3* in TNBC cells, loss-of-function assays using siRNA were performed. We evaluated

Table 2 Candidate target genes regulated by *miR-204-5p* in BC cells

Entrez GeneID	Gene Symbol	Gene name	target sites		Gene expression	mRNA profile	TCGA OncoLnc
			Conserved	Poorly	FC (log)	FC (log)	p-value
130340	*AP1S3*	adaptor-related protein complex 1, sigma 3 subunit	0	2	−3.413969	2.086208136	0.00823
5806	*PTX3*	pentraxin 3, long	0	1	−1.0041008	1.90440246	0.0215
29127	*RACGAP1*	Rac GTPase activating protein 1	0	1	−1.0164127	3.2363117	0.0277
79071	*ELOVL6*	ELOVL fatty acid elongase 6	1	2	−1.0130367	1.11074909	0.0448
55379	*LRRC59*	leucine rich repeat containing 59	0	2	−1.0145847	2.10652314	0.0456
7374	*UNG*	uracil-DNA glycosylase	0	1	−1.7226859	1.80758974	0.0651
51373	*MRPS17*	28S ribosomal protein S17, mitochondrial; HCG1984214, isoform CRA_a	1	0	−2.460019	1.361706337	0.0695
56829	*ZC3HAV1*	zinc finger CCCH-type, antiviral 1	0	2	−1.1792603	1.64439738	0.102
10267	*RAMP1*	receptor (G protein-coupled) activity modifying protein 1	0	1	−1.3744812	2.767818624	0.114
55143	*CDCA8*	cell division cycle associated 8	0	2	−1.3121843	5.585709686	0.137
7851	*MALL*	mal, T-cell differentiation protein-like	1	1	−1.0069504	1.05029346	0.195
7456	*WIPF1*	WAS/WASL interacting protein family, member 1	0	1	−1.1285505	1.886397	0.196
7058	*THBS2*	thrombospondin 2	1	0	−1.594156	1.294138334	0.209
388507	*ZNF788*	zinc finger family member 788	0	1	−1.6381234	1.92002958	0.234
51714	*SELT*	Selenoprotein T	0	1	−1.2179046	1.12461617	0.295
51465	*UBE2J1*	ubiquitin-conjugating enzyme E2, J1	1	2	−1.0475721	1.8167851	0.432
53339	*BTBD1*	BTB (POZ) domain containing 1	1	1	−2.4108038	1.1226325	0.476
860	*RUNX2*	runt-related transcription factor 2	1	3	−1.117322	1.4735198	0.483
1009	*CDH11*	cadherin 11, type 2, OB-cadherin (osteoblast)	1	0	−1.1122861	1.97772899	0.495
1174	*AP1S1*	adaptor-related protein complex 1, sigma 1 subunit	1	0	−1.4767408	1.338973895	0.496
374383	*NCR3LG1*	natural killer cell cytotoxicity receptor 3 ligand 1	0	6	−1.0475403	1.990964203	0.567
6749	*SSRP1*	structure specific recognition protein 1	1	0	−1.3913507	1.399509792	0.579
5308	*PITX2*	paired-like homeodomain 2	0	2	−1.0198526	1.129093126	0.653
8886	*DDX18*	DEAD (Asp-Glu-Ala-Asp) box polypeptide 18	1	0	−1.0809115	1.026206295	0.657
1371	*CPOX*	coproporphyrinogen oxidase	1	0	−1.5116881	1.13203495	0.669
201725	*C4orf46*	chromosome 4 open reading frame 46	0	1	−1.4400569	1.742180231	0.72
83463	*MXD3*	MAX dimerization protein 3	0	1	−1.2148519	2.038010365	0.739
5795	*PTPRJ*	protein tyrosine phosphatase, receptor type, J	1	1	−1.1419544	1.66329295	0.8
84002	*B3GNT5*	UDP-GlcNAc:betaGal beta-1,3-N-acetylglucosaminyltransferase 5	1	1	−1.3670406	1.2560426	0.827
79056	*PRRG4*	proline rich Gla (G-carboxyglutamic acid) 4 (transmembrane)	0	1	−1.0532522	1.53708755	0.874
8905	*AP1S2*	adaptor-related protein complex 1, sigma 2 subunit	2	0	−2.466689	1.25244963	0.934
56935	*SMCO4*	single-pass membrane protein with coiled-coil domains 4	0	1	−1.1516161	1.24182446	0.981

the knockdown efficiency of si-*AP1S3*-transfected TNBC cell lines. Downregulation of *AP1S3*/AP1S3 was detected in si-*AP1S3* transfectants (Fig. 3a, b).

Cancer cell proliferation, migration, and invasion were significantly reduced in si-*AP1S3* transfectants compared with those in mock- or miR-control-transfected TNBC cell lines (Fig. 3c–e).

In addition, we investigated the oncogenic roles of *AP1S3* by using other cancer cell lines (MDA-MB157: breast cancer and H1299: lung adenocarcinoma). A large

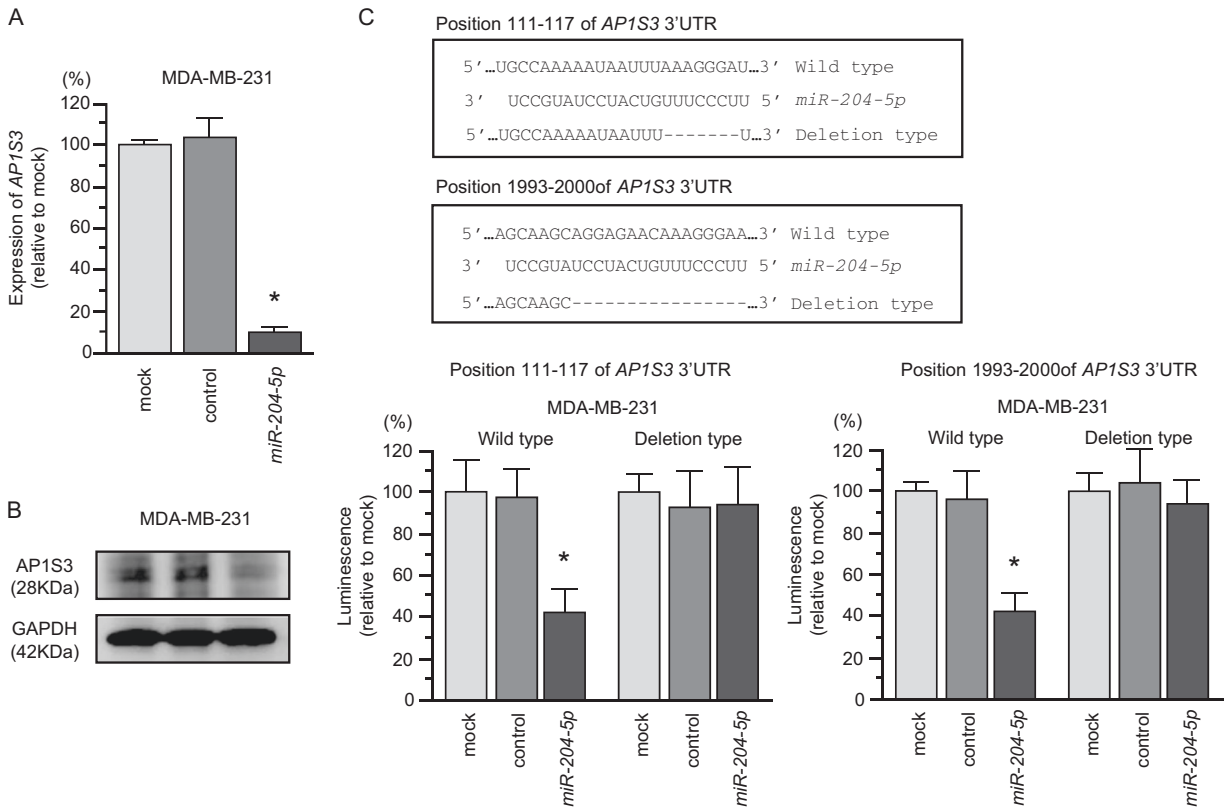

Fig. 2 Direct regulation of *AP1S3* by *miR-204-5p* in BC cells. **a** Expression levels of *AP1S3* mRNA 72 h after transfection with 10 nM *miR-204-5p* into cell line. *GUSB* was used as an internal control. *$p <$ 0.0001. **b** Expression of AP1S3 protein 96 h after transfection with *miR-204-5p*. GAPDH was used as a loading control. **c** *miR-204-5p* binding sites in the 3′-untranslated region (3′-UTR) of *AP1S3* mRNA. Dual-luciferase reporter assays using vectors encoding putative *miR-204-5p* target sites (positions 111−117 or 1993−2000) in the *AP1S3* 3′-UTR for both wild-type and deleted regions. *Renilla* luciferase values were normalized to firefly luciferase values. *$p < 0.005$

number of cohort analyses by TCGA datasets showed that high expression of *AP1S3* significantly predicted poor prognosis of lung adenocarcinoma (Supplementary Fig. 4A). Our functional assays showed that cancer cell aggressiveness was markedly suppressed by transfecting with si-*AP1S3* into MDA-MB-157 and H1299 cell lines (Supplementary Fig. 4B).

Expression of *AP1S3* in BC clinical specimens and its clinical significance

AP1S3 expression levels were significantly upregulated in TNBC tissues (Fig. 4a). Spearman's rank tests showed a negative correlation between the expression of *AP1S3* and *miR-204-5p* ($p = 0.0129$, $r = -0.488$; Fig. 4b). Based on the TCGA database analysis, the overall survival rates of patients with BC were significantly shorter in patients with elevated *AP1S3* expression compared with those in patients with low expression ($p = 0.00823$; Fig. 4c).

Finally, we performed univariate and multivariate Cox hazard regression analyses to investigate the clinical significance of *AP1S3* expression for overall survival in patients with BC. After multivariate analysis, high *AP1S3* expression levels, age (>60 years), lymph node metastasis status, and metastasis status were found to be independent predictive factors for overall survival (hazard ratio (HR) = 1.77, $p = 0.0031$; HR = 2.02, $p = 0.0004$; HR = 2.18, $p = 0.0002$; and HR = 3.19, $p = 0.0017$, respectively; Supplementary Table 3). These findings showed that overexpression of *AP1S3* was relevant to cancer aggressiveness and was associated with poor outcomes.

Further examination of the protein expression levels of AP1S3 in TNBC clinical specimens by immunostaining showed that AP1S3 was strongly expressed in cancer lesions, but not in noncancerous epithelial tissues (Fig. 4d).

Downstream genes affected by silencing of *AP1S3* in BC cells

To identity downstream genes regulated by *AP1S3*, we used genome-wide gene expression data (si-*AP1S3*-transfected cells and TNBC expression data). In total, 32 genes were identified as putative downstream genes regulated by

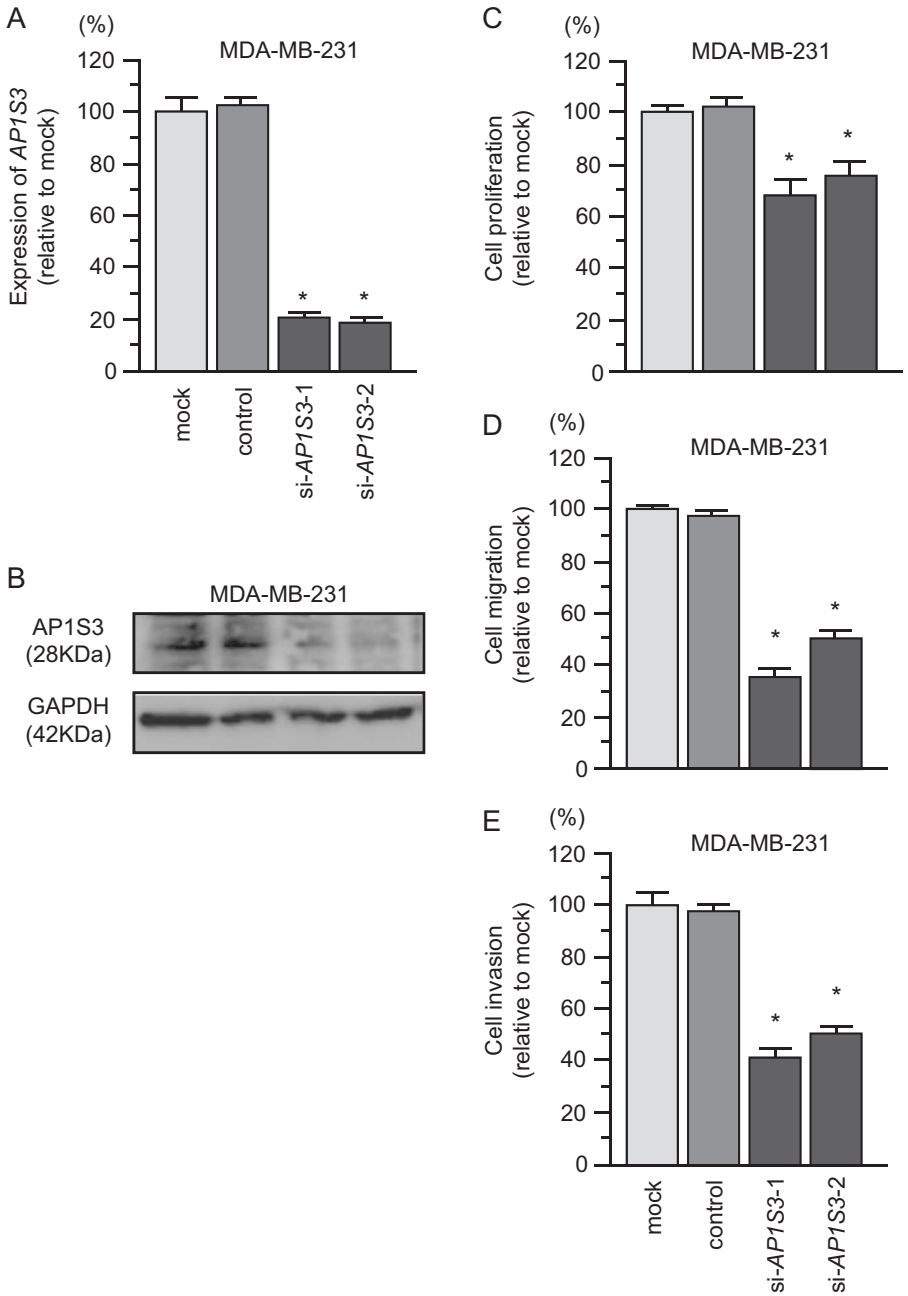

Fig. 3 Effects of silencing *AP1S3* in BC cells. **a** *AP1S3* mRNA expression 72 h after transfection of BC cells with 10 nM si-*AP1S3*. *GUSB* was used as an internal control. *$p < 0.0001$. **b** AP1S3 protein expression 96 h after transfection with si-*AP1S3*. GAPDH was used as a loading control. **c** Cell proliferation was determined with XTT assays 72 h after transfection with 10 nM si-*AP1S3*. *$p < 0.0001$. **d** Results of cell migration assays. *$p < 0.0001$. **e** Results of Matrigel invasion assays. *$p < 0.0001$

AP1S3 in BC cells (Supplementary Table 4). Expression data were deposited into GEO (https://www.ncbi.nlm.nih.gov/geo/), with accession number GSE115909.

Discussion

Recent studies associated with the Human Genome Project have revealed that in human cells, various RNAs (protein-coding RNAs, small noncoding RNAs, and large noncoding RNAs) form complicated RNA networks and are responsible for many biological processes [25]. Disruption of tightly regulated RNA networks by aberrantly expressed miRNAs contributes to cancer cell development, metastasis, and drug resistance [26, 27]. Therefore, the identification of miRNAs that are abnormally expressed in cancer cells will facilitate the search for novel RNA networks in cancer cells. To search for miRNAs characteristic of cancer cells, we

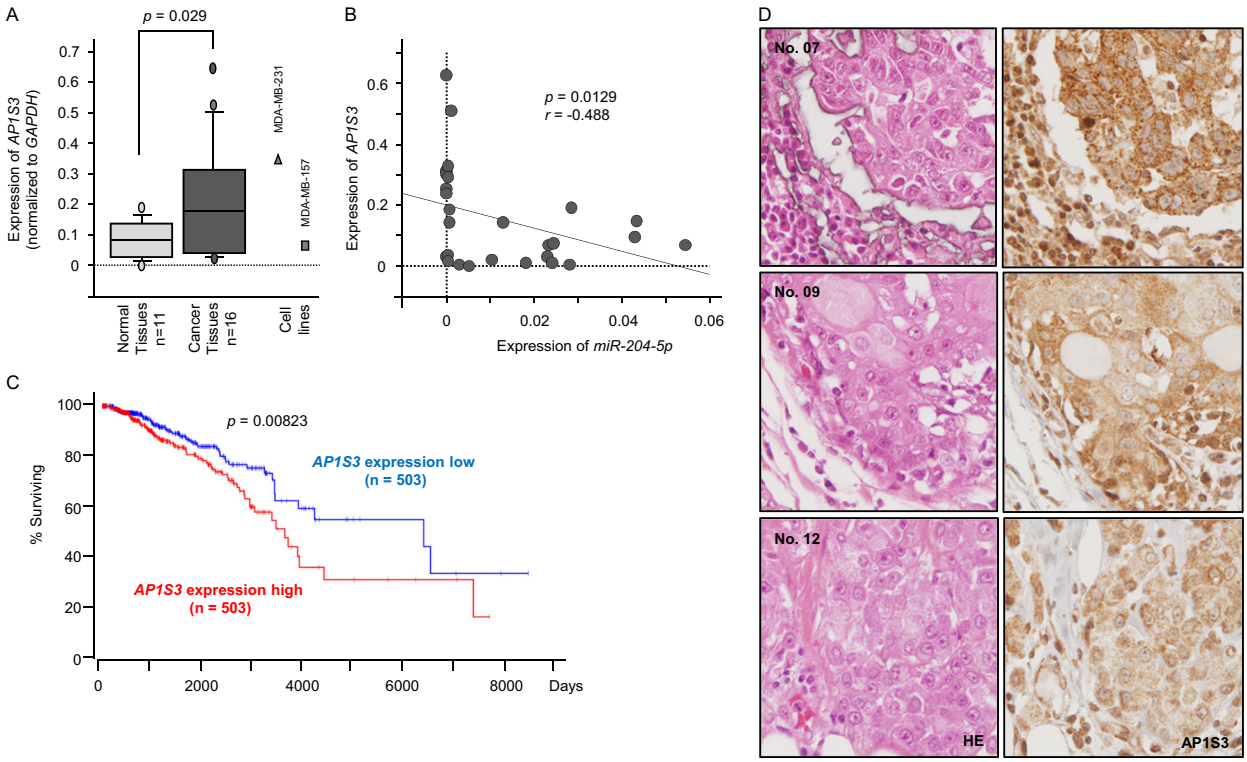

Fig. 4 Expression of *AP1S3* in TNBC clinical specimens. **a** Expression levels of *AP1S3* in TNBC clinical specimens. *GUSB* was used as an internal control. **b** Spearman's rank test was used to evaluate the correlations between *AP1S3* expression and *miR-204-5p*. **c** The 5-year survival rates were analyzed by Kaplan−Meier survival curves and log-rank statistics. **d** Immunostaining showed that AP1S3 was strongly expressed in cancer lesions, but not in noncancerous epithelial tissues

created miRNA expression signatures using clinical specimens from patients with several types of cancers based on the most advanced genomic strategies [16–19, 28–30].

In this study, we created a novel TNBC miRNA expression signature by RNA sequencing and found that 104 miRNAs (56 upregulated and 48 downregulated) were dysregulated in TNBC tissues. Importantly, some passenger strands of miRNAs were aberrantly expressed in cancer tissues, e.g., *miR-202-5p*, *miR-99a-3p*, *miR-675-3p*, *miR-10b-3p*, *miR-145-3p*, and *miR-30a-3p*. It is generally believed that the passenger strands of miRNAs are degraded and therefore have no function [31, 32]. However, our recent studies have shown that *miR-99a-3p* and *miR-145-3p* act as antitumor miRNAs by targeting several oncogenes, including *MELK*, *NCAPG*, *BUB1*, and *CDK1*, in prostate cancer [17, 33]. The involvement of passenger strands of miRNAs in cancer pathogenesis is a new concept of cancer research. The miRNA signature we obtained in this study represents a major advancement in TNBC research and is expected to facilitate the identification of novel RNA networks associated with the aggressiveness of TNBC.

In the present study, we focused on *miR-204-5p* because its expression showed the greatest downregulation in TNBC tissues in our signature. Our present data showed that ectopic expression of *miR-204-5p* inhibited processes associated with cancer cell malignancy, suggesting that this miRNA had antitumor effects in BC cells. Previous studies have demonstrated that *miR-204-5p* acts as an antitumor miRNA in several cancers [34–37]. In BC cells, the expression of *miR-204-5p* has been shown to suppress the epithelial–mesenchymal transition (EMT) phenotype in cancer cells by targeting the homeobox protein sineoculis homeobox homolog 1 (*SIX1*) [38]. Overexpression of SIX1 was observed in BC and was found to be related to BC cell metastasis by promoting the EMT [39]. Further studies of such miRNA-regulated molecular networks will contribute to the identification of molecular mechanisms mediating carcinogenesis.

We also attempted to identify RNA networks regulated by *miR-204-5p* in BC cells. Our in silico and genome-wide gene expression analyses revealed 32 candidate oncogenes that may be controlled by *miR-204-5p* in TNBC cells. Among these targets, four overexpressed genes (*AP1S3*: $p = 0.00823$, *RACGAP1*: $p = 0.0277$, *ELOVL6*: $p = 0.0448$, and *LRRC59*: $p = 0.0456$) were predicted to be associated with poor prognosis in patients with BC in TCGA database. Rac GTPase-activating protein 1 (*RACGAP1*) binds the activated form of Rho GTPase and stimulates GTP hydrolysis, resulting in negative regulation of Rho-mediated signals. Several studies have shown that expression of

RACGAP1 is directly correlated with shorter disease-free survival in patients with BC [40–42]. Moreover, RACGAP1 was found to behave as an oncogene in BC cells. Functional analysis of these target genes will be helpful for improving our understanding of the molecular pathology of TNBC.

In this study, we focused on *AP1S3* because its expression was associated with poor prognosis in patients with BC. In addition, no studies have examined the relationship between *AP1S3* and cancer pathogenesis. AP1S3 is a component of adaptor protein complex 1 (AP-1), and three paralogous genes, *AP1S1*, *AP1S2*, and *AP1S3* exist in the human genome [43]. AP1S proteins are essential for the stability of the AP-1 complex, and mutation of *AP1S* genes may disrupt the AP-1 complex. AP-1 complexes are involved in clathrin-mediated vesicular transport from the Golgi or endosomes [44]. Moreover, the AP-1 complex has been implicated in the formation of autophagosomes [45]. In a recent study, mutations in the *AP1S3* gene were identified in patients with pustular psoriasis, a severe autoinflammatory skin disorder [46, 47]. To the best of our knowledge, this is the first report demonstrating that *AP1S3* was directly regulated by antitumor *miR-204-5*p and that expression of *AP1S3* was involved in cancer pathogenesis. Interestingly, other *AP1S* members, i.e., *AP1S1* and *AP1S2*, were identified as *miR-204-5p*-regulated targets in TNBC cells. Further studies are needed to determine how aberrant expression of these genes is involved in cancer development.

To investigate the biological significance of *AP1S3* in BC cells, we investigated the downstream genes modulated by *AP1S3*. A total of 33 putative target genes were downregulated by transfecting with si-*AP1S3* into BC cells. These genes will be useful for understanding molecular pathogenesis of *AP1S3*-modulated BC cells. For example, *YWHAZ*, a member of the 14-3-3 family was high expression of BC clinical specimens and its aberrant expression contributed to chemotherapy resistance and recurrence of BC [48–50]. More recently, *miR-451* was downregulated in paclitaxel-resistant BC cells and *YWHAZ* was a direct target of *miR-451* in BC cells [51]. Interestingly, our miRNA signature of TNBC showed that *miR-451a* was significantly downregulated in cancer tissues. Further studies of antitumor miRNA-modulated molecular pathways in TNBC may provide novel insights into the molecular pathogenesis of this disease.

In conclusion, dysregulated miRNAs, including passenger strands of miRNAs, were successfully identified by RNA sequencing-based signatures in TNBC cells. Downregulation of *miR-204-5p* was detected by our present signature, and this miRNA was found to function as an antitumor miRNA in TNBC cells. Direct regulation of *AP1S3* by *miR-204-5p* was detected in BC cells, and *AP1S3* expression was found to be involved in BC pathogenesis. Identification of novel cancer networks mediated by aberrantly expressed miRNAs may improve our understanding of the molecular pathogenesis of TNBC. Moreover, our newly created RNA sequencing-based miRNA signature establishes a basis for further TNBC research.

Acknowledgements The present study was supported by KAKENHI grants 15K10801, 18K09338, 16K19906, 17H04285, 16K10465 and 18K16322.

Compliance with ethical standards

Conflict of interest The authors declare that they have no conflict of interest

References

1. Torre LA, Bray F, Siegel RL, Ferlay J, Lortet-Tieulent J, Jemal A. Global cancer statistics, 2012. CA Cancer J Clin. 2015;65:87–108.
2. Koboldt DC, Fulton RS, McLellan MD, Schmidt H, Kalicki-Veizer J, McMichael JF, et al. Comprehensive molecular portraits of human breast tumours. Nature. 2012;490:61–70.
3. Perou CM, Sorlie T, Eisen MB, van de Rijn M, Jeffrey SS, Rees CA, et al. Molecular portraits of human breast tumours. Nature. 2000;406:747–52.
4. Coates AS, Winer EP, Goldhirsch A, Gelber RD, Gnant M, Piccart-Gebhart M, et al. Tailoring therapies—improving the management of early breast cancer: St Gallen International Expert Consensus on the Primary Therapy of Early Breast Cancer 2015. Ann Oncol. 2015;26:1533–46.
5. Goldhirsch A, Winer EP, Coates AS, Gelber RD, Piccart-Gebhart M, Thurlimann B, et al. Personalizing the treatment of women with early breast cancer: highlights of the St Gallen International Expert Consensus on the Primary Therapy of Early Breast Cancer 2013. Ann Oncol. 2013;24:2206–23.
6. Foulkes WD, Smith IE, Reis-Filho JS. Triple-negative breast cancer. N Engl J Med. 2010;363:1938–48.
7. Poggio F, Bruzzone M, Ceppi M, Ponde NF, La Valle G, Del Mastro L, et al. Platinum-based neoadjuvant chemotherapy in triple-negative breast cancer: a systematic review and meta-analysis. Ann Oncol. 2018;29:1497–508.
8. Bartel DP. MicroRNAs: target recognition and regulatory functions. Cell. 2009;136:215–33.
9. Guo H, Ingolia NT, Weissman JS, Bartel DP. Mammalian microRNAs predominantly act to decrease target mRNA levels. Nature. 2010;466:835–40.
10. He L, He X, Lowe SW, Hannon GJ. microRNAs join the p53 network—another piece in the tumour-suppression puzzle. Nat Rev Cancer. 2007;7:819–22.
11. Shenoy A, Blelloch RH. Regulation of microRNA function in somatic stem cell proliferation and differentiation. Nat Rev Mol Cell Biol. 2014;15:565–76.
12. Lin S, Gregory RI. MicroRNA biogenesis pathways in cancer. Nat Rev Cancer. 2015;15:321–33.
13. Rupaimoole R, Slack FJ. MicroRNA therapeutics: towards a new era for the management of cancer and other diseases. Nat Rev Drug Discov. 2017;16:203–22.
14. Kurozumi S, Yamaguchi Y, Kurosumi M, Ohira M, Matsumoto H, Horiguchi J. Recent trends in microRNA research into breast cancer with particular focus on the associations between microRNAs and intrinsic subtypes. J Hum Genet. 2017;62:15–24.

15. Filipowicz W, Bhattacharyya SN, Sonenberg N. Mechanisms of post-transcriptional regulation by microRNAs: are the answers in sight? Nat Rev Genet. 2008;9:102–14.
16. Itesako T, Seki N, Yoshino H, Chiyomaru T, Yamasaki T, Hidaka H, et al. The microRNA expression signature of bladder cancer by deep sequencing: the functional significance of the miR-195/497 cluster. PLoS ONE. 2014;9:e84311.
17. Goto Y, Kurozumi A, Arai T, Nohata N, Kojima S, Okato A, et al. Impact of novel miR-145-3p regulatory networks on survival in patients with castration-resistant prostate cancer. Br J Cancer. 2017;117:409–20.
18. Yonemori K, Seki N, Idichi T, Kurahara H, Osako Y, Koshizuka K, et al. The microRNA expression signature of pancreatic ductal adenocarcinoma by RNA sequencing: anti-tumour functions of the microRNA-216 cluster. Oncotarget. 2017;8:70097–115.
19. Koshizuka K, Nohata N, Hanazawa T, Kikkawa N, Arai T, Okato A, et al. Deep sequencing-based microRNA expression signatures in head and neck squamous cell carcinoma: dual strands of pre-miR-150 as antitumor miRNAs. Oncotarget. 2017;8:30288–304.
20. Arai T, Fuse M, Goto Y, Kaga K, Kurozumi A, Yamada Y, et al. Molecular pathogenesis of interstitial cystitis based on microRNA expression signature: miR-320 family-regulated molecular pathways and targets. J Hum Genet. 2018;63:543–54.
21. Idichi T, Seki N, Kurahara H, Yonemori K, Osako Y, Arai T, et al. Regulation of actin-binding protein ANLN by antitumor miR-217 inhibits cancer cell aggressiveness in pancreatic ductal adenocarcinoma. Oncotarget. 2017;8:53180–93.
22. Idichi T, Seki N, Kurahara H, Fukuhisa H, Toda H, Shimonosono M, et al. Molecular pathogenesis of pancreatic ductal adenocarcinoma: impact of passenger strand of pre-miR-148a on gene regulation. Cancer Sci. 2018;109:2013–26.
23. Idichi T, Seki N, Kurahara H, Fukuhisa H, Toda H, Shimonosono M, et al. Involvement of anti-tumor miR-124-3p and its targets in the pathogenesis of pancreatic ductal adenocarcinoma: direct regulation of ITGA3 and ITGB1 by miR-124-3p. Oncotarget. 2018;9:28849–65.
24. Yamada Y, Arai T, Sugawara S, Okato A, Kato M, Kojima S, et al. Impact of novel oncogenic pathways regulated by antitumor miR-451a in renal cell carcinoma. Cancer Sci. 2018;109:1239–53.
25. Anastasiadou E, Jacob LS, Slack FJ. Non-coding RNA networks in cancer. Nat Rev Cancer. 2018;18:5–18.
26. Koshizuka K, Hanazawa T, Arai T, Okato A, Kikkawa N, Seki N. Involvement of aberrantly expressed microRNAs in the pathogenesis of head and neck squamous cell carcinoma. Cancer Metastas- Rev. 2017;36:525–45.
27. Azmi AS, Bao B, Sarkar FH. Exosomes in cancer development, metastasis, and drug resistance: a comprehensive review. Cancer Metastas- Rev. 2013;32:623–42.
28. Goto Y, Kurozumi A, Nohata N, Kojima S, Matsushita R, Yoshino H, et al. The microRNA signature of patients with sunitinib failure: regulation of UHRF1 pathways by microRNA-101 in renal cell carcinoma. Oncotarget. 2016;7:59070–86.
29. Goto Y, Kojima S, Nishikawa R, Kurozumi A, Kato M, Enokida H, et al. MicroRNA expression signature of castration-resistant prostate cancer: the microRNA-221/222 cluster functions as a tumour suppressor and disease progression marker. Br J Cancer. 2015;113:1055–65.
30. Mizuno K, Mataki H, Arai T, Okato A, Kamikawaji K, Kumamoto T, et al. The microRNA expression signature of small cell lung cancer: tumor suppressors of miR-27a-5p and miR-34b-3p and their targeted oncogenes. J Hum Genet. 2017;62:671–8.
31. Peschansky VJ, Wahlestedt C. Non-coding RNAs as direct and indirect modulators of epigenetic regulation. Epigenetics. 2014;9:3–12.
32. Adams BD, Kasinski AL, Slack FJ. Aberrant regulation and function of microRNAs in cancer. Curr Biol. 2014;24:R762–776.
33. Arai T, Okato A, Yamada Y, Sugawara S, Kurozumi A, Kojima S, et al. Regulation of NCAPG by miR-99a-3p (passenger strand) inhibits cancer cell aggressiveness and is involved in CRPC. Cancer Med. 2018;7:1988–2002.
34. Chung TK, Lau TS, Cheung TH, Yim SF, Lo KW, Siu NS, et al. Dysregulation of microRNA-204 mediates migration and invasion of endometrial cancer by regulating FOXC1. Int J Cancer. 2012;130:1036–45.
35. Ding M, Lin B, Li T, Liu Y, Li Y, Zhou X, et al. A dual yet opposite growth-regulating function of miR-204 and its target XRN1 in prostate adenocarcinoma cells and neuroendocrine-like prostate cancer cells. Oncotarget. 2015;6:7686–7700.
36. Shi L, Zhang B, Sun X, Lu S, Liu Z, Liu Y, et al. MiR-204 inhibits human NSCLC metastasis through suppression of NUAK1. Br J Cancer. 2014;111:2316–27.
37. Yin Y, Zhang B, Wang W, Fei B, Quan C, Zhang J, et al. miR-204-5p inhibits proliferation and invasion and enhances chemotherapeutic sensitivity of colorectal cancer cells by down-regulating RAB22A. Clin Cancer Res. 2014;20:6187–99.
38. Zeng J, Wei M, Shi R, Cai C, Liu X, Li T, et al. MiR-204-5p/Six1 feedback loop promotes epithelial−mesenchymal transition in breast cancer. Tumour Biol. 2016;37:2729–35.
39. Micalizzi DS, Christensen KL, Jedlicka P, Coletta RD, Baron AE, Harrell JC, et al. The Six1 homeoprotein induces human mammary carcinoma cells to undergo epithelial-mesenchymal transition and metastasis in mice through increasing TGF-beta signaling. J Clin Invest. 2009;119:2678–90.
40. Pliarchopoulou K, Kalogeras KT, Kronenwett R, Wirtz RM, Eleftheraki AG, Batistatou A, et al. Prognostic significance of RACGAP1 mRNA expression in high-risk early breast cancer: a study in primary tumors of breast cancer patients participating in a randomized Hellenic Cooperative Oncology Group trial. Cancer Chemother Pharmacol. 2013;71:245–55.
41. Milde-Langosch K, Karn T, Muller V, Witzel I, Rody A, Schmidt M, et al. Validity of the proliferation markers Ki67, TOP2A, and RacGAP1 in molecular subgroups of breast cancer. Breast Cancer Res Treat. 2013;137:57–67.
42. Kotoula V, Kalogeras KT, Kouvatseas G, Televantou D, Kronenwett R, Wirtz RM, et al. Sample parameters affecting the clinical relevance of RNA biomarkers in translational breast cancer research. Virchows Arch. 2013;462:141–54.
43. Glyvuk N, Tsytsyura Y, Geumann C, D'Hooge R, Huve J, Kratzke M, et al. AP-1/sigma1B-adaptin mediates endosomal synaptic vesicle recycling, learning and memory. EMBO J. 2010;29:1318–30.
44. Robinson MS, Bonifacino JS. Adaptor-related proteins. Curr Opin Cell Biol. 2001;13:444–53.
45. Ko SH, Jeon JI, Myung HS, Kim YJ, Kim JM. *Bacteroides fragilis* enterotoxin induces formation of autophagosomes in endothelial cells but interferes with fusion with lysosomes for complete autophagic flux through a mitogen-activated protein kinase-, AP-1-, and C/EBP homologous protein-dependent pathway. Infect Immun. 2017;85:e00420–17.
46. Setta-Kaffetzi N, Simpson MA, Navarini AA, Patel VM, Lu HC, Allen MH, et al. AP1S3 mutations are associated with pustular psoriasis and impaired Toll-like receptor 3 trafficking. Am J Hum Genet. 2014;94:790–7.
47. Mahil SK, Twelves S, Farkas K, Setta-Kaffetzi N, Burden AD, Gach JE, et al. AP1S3 mutations cause skin autoinflammation by disrupting keratinocyte autophagy and up-regulating IL-36 production. J Invest Dermatol. 2016;136:2251–9.

48. Frasor J, Chang EC, Komm B, Lin CY, Vega VB, Liu ET, et al. Gene expression preferentially regulated by tamoxifen in breast cancer cells and correlations with clinical outcome. Cancer Res. 2006;66:7334–40.
49. Li Y, Zou L, Li Q, Haibe-Kains B, Tian R, Li Y, Desmedt C, et al. Amplification of LAPTM4B and YWHAZ contributes to chemotherapy resistance and recurrence of breast cancer. Nat Med. 2010;16:214–8.
50. Bergamaschi A, Christensen BL, Katzenellenbogen BS. Reversal of endocrine resistance in breast cancer: interrelationships among 14-3-3ζ, FOXM1, and a gene signature associated with mitosis. Breast Cancer Res. 2011;13:R70.
51. Wang W, Zhang L, Wang Y, Ding Y, Chen T, Wang Y, et al. Involvement of miR-451 in resistance to paclitaxel by regulating YWHAZ in breast cancer. Cell Death Dis. 2017;8:e3071.